Spin-splitting in an $Al_xGa_{1-x}N/GaN$ nanowire for a quantum-ring interferometer

Ikai Lo,[1,a)] Wen-Yuan Pang,[1] Yen-Liang Chen,[1] Yu-Chi Hsu,[1] Jih-Chen Chiang,[1] Wei-Hsin Lin,[1] Wan-Ting Chiu,[1] Jenn-Kai Tsai,[2] and Chun-Nan Chen[3]
[1]*Department of Physics, Center for Nanoscience and Nanotechnology, National Sun Yat-Sen University, Kaohsiung, 80424 Taiwan, Republic of China*
[2]*National Formosa University, Hu-Wei, Yun-Lin County, 63201 Taiwan, Republic of China*
[3]*Department of Physics, Tamkang University, Tamsui, Taipei County, 25137 Taiwan, Republic of China*

(Received 29 July 2008; accepted 15 September 2008; published online 3 October 2008)

An $Al_{0.18}Ga_{0.82}N/GaN$ heterostructure was used to fabricate a ballistic nanowire with a wire width of 200 nm by focused ion beam. We observed the beating Shubnikov–de Haas oscillations in the nanowire with a spin-splitting energy of (2.4 ± 0.3) meV. Based on the results, we proposed a spin-Hall quantum-ring interferometer made of $Al_xGa_{1-x}N/GaN$ nanowires for spintronic applications. © *2008 American Institute of Physics*. [DOI: 10.1063/1.2995866]

Since the Aharonov–Bohm effect was observed in metallic rings,[1,2] the effect has been applied to InGaAs/AlInAs quantum-ring semiconductors for device application.[3–5] It originated from the periodic dependence of electron wave function on magnetic flux (h/e) penetrating a ring, leading to an oscillatory behavior in the electron energy levels as a function of the applied magnetic field.[6] Currently, it attracted more attention to spin-sensitive devices, in which spin-orbit interaction is the main mechanism for the spin transportation.[7] The spin-orbit interaction gives rise to a Rashba effect (due to the structural inversion asymmetry of confinement potential at heterointerface) and a Dresselhaus effect (with a bulk inversion asymmetry of crystal potential) in zinc-blende semiconductors (e.g., InGaAs/AlInAs). A long lifetime spin-current is expected in the spin-degenerate case as the Rashba and Dresselhaus effects are equal.[8] Moreover, the spin-orbit interaction will induce a spin-Hall effect in a heterostructure with a Rashba term such as InGaAs/AlInAs, leading to a spin accumulation at the sample boundaries.[9] Besides, Lo *et al.*[10] observed a large spin-splitting of a two-dimensional electron gas (2DEG) in a wurtzite AlGaN/GaN heterostructure, which made the GaN-based heterostructure a promising candidate for the spintronic application. The Hamiltonian of the spin-orbit interaction in GaN shows an isotropic character due to the wurtzite structure effect: $\boldsymbol{H}_{so} = [\alpha_{wz} - \gamma_{wz}(bk_z^2 - k_\parallel^2)](\sigma_x k_y - \sigma_y k_x)$, where α_{wz} is the coupling coefficient of the Rashba effect plus intrinsic wurtzite linear-$\boldsymbol{k}$ term and γ_{wz} is the coefficient of Dresselhaus cubic-$\boldsymbol{k}$ term (here the lattice parameter $b=4$ for an ideal wurtzite).[11] The Hamiltonian yields a spin-degenerate Fermi surface,[12] if $[\alpha_{wz} - \gamma_{wz}(bk_z^2 - k_\parallel^2)] = 0$. Spin-degenerate Fermi surfaces have been observed in AlGaN/GaN heterostructures.[11] Therefore, the quantum-ring interferometer can be designed with a specified dimension on AlGaN/GaN heterostructure. For instance in Fig. 1(a), the dimension of the leads for source and drain (the green regions) is wide enough to form a 2DEG for the spin-Hall effect, but the wire width of the ring (the blue area) is reduced to the electron mean free path for ballistic transportation. The Rashba spin-splitting between spin-up and spin-down electrons can be used to control the differential phase shift of the electrons by an electric field, leading to the modulation control of the electrons even in the absence of a magnetic field. By applying an electric field to the semiconductor 2D channel, the electrons of spin-up go to one edge and those of spin-down go to the opposite one, resulting in a transverse flow of spin.[13] When the spin-Hall effect is allowed to produce spin-polarized 2DEG currents along the edges of source lead, (i.e., $|\psi_S\rangle$, which consists of spin-down electrons $|\psi_\downarrow\rangle$ moving

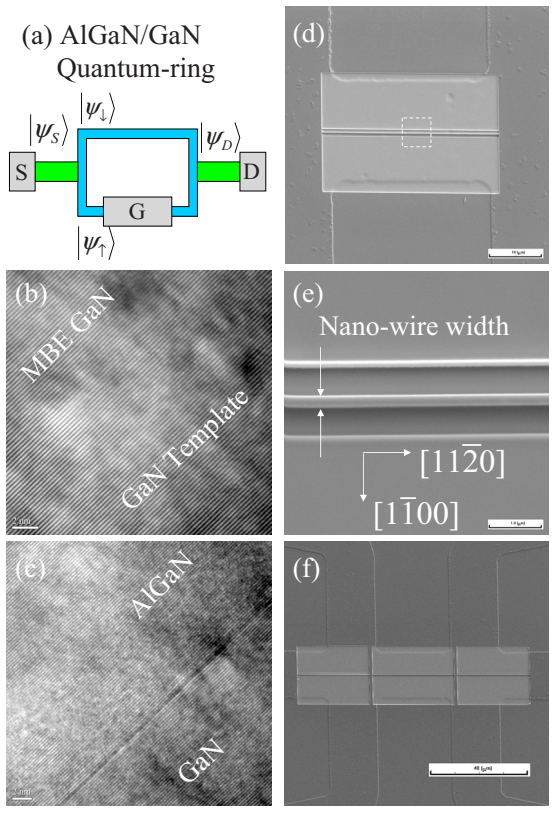

FIG. 1. (Color online) (a) The proposed AlGaN/GaN quantum-ring interferometer. (b) TEM micrographs taken at the area between MBE GaN and GaN template and (c) at AlGaN/GaN heterointerface. (d) The SEM image of nanowire fabricated by FIB lithography. (e) The enlarged image of the dotted area of (d). (f) The final pattern of the nanowires. The scale bars are 2 nm for (b) and (c), 10 μm for (d), 1 μm for (e), and 40 μm for (f).

a)Electronic mail: ikailo@mail.phys.nsysu.edu.tw.

along the upper edge and spin-up electrons $|\psi_{\uparrow}\rangle$ along the lower edge), the 2D spin-polarized currents will individually flow into or out of the quantum ring via separated nanowire arms. Thereafter, the spin-down electrons ($|\psi_{\downarrow}\rangle$) move to the upper nongated arm but the spin-up electrons ($|\psi_{\uparrow}\rangle$) go through the lower gated arm, and both are detected by the 2D drain lead ($|\psi_D\rangle$). If the width of the nanowire is much smaller than the electron mean free path (i.e., a ballistic transportation), the scattering of electron will be minimized and the quantum states of the spin-polarized currents are conserved in the nanowire arms. Because the spin splitting in the gated arm can be modulated by an electric field due to Rashba effect, a low-power spin-Hall quantum-ring interferometer is then obtained by tuning the gate voltage. In this letter, we demonstrate a spin-splitting in AlGaN/GaN ballistic nanowire for the application of spin interferometer.

The $Al_xGa_{1-x}N/GaN$ heterostructure was grown on a 3 μm GaN-template using plasma-assisted molecular beam epitaxy (MBE). The GaN-template was prepared by metal-organic vapor phase epitaxy on (0001) sapphire, and the heterostructure was grown with a Ga/N flux ratio (beam equivalent pressure) of 5.3 at 850 °C in the sequence: 600 nm undoped GaN, 15 nm $Al_{0.18}Ga_{0.82}N$ spacer, 15 nm Si-doped $Al_{0.18}Ga_{0.82}N$, and 15 nm undoped $Al_{0.18}Ga_{0.82}N$ cap. The cross-sectional image of the high-resolution transmission electron microscopy (TEM) shows that the MBE GaN was well developed onto the template, Fig. 1(b), and the heterointerface of $Al_{0.18}Ga_{0.82}N/GaN$ is clearly visible in Fig. 1(c). To evaluate the carrier property, we performed a van der Pauw Hall measurement at the temperature of 77 K on a square sample of 5×5 mm^2 cut from the $Al_{0.18}Ga_{0.82}N/GaN$ heterostructure. We obtained the mobility and carrier density to be 9300 cm^2/V s and 7.86×10^{12} cm^{-2}, respectively. To evaluate the 2DEG of the sample, we calculated the band profile of the heterostructure by the solutions of Poisson–Schrödinger equations,[14] assuming that the carriers are entirely excited from the shallow donors located at the $Al_{0.18}Ga_{0.82}N$ barrier. The result is shown in the inset of Fig. 2(b). We obtained that the separation between the first two subbands is $E_2-E_1=83$ meV. The sheet carrier concentration (n_s) exhibits a major peak at $\langle z\rangle=0.8$ nm from the heterointerface and a secondary peak is located at the $Al_{0.18}Ga_{0.82}N$ barrier. The ratio of the carrier concentration residing at GaN layer versus that at $Al_{0.18}Ga_{0.82}N$ barrier is (7.025: 1), yielding $n_{2d}\approx6.88\times10^{12}$ cm^{-2} at the heterointerface and 0.98×10^{12} cm^{-2} at the $Al_{0.18}Ga_{0.82}N$ barrier. Using the effective mass $m^*=0.215m_0$,[11] we calculated the Fermi level to be 76.6 meV above the first subband minimum and its Fermi wave vector $k_F=0.6575$ nm^{-1} (or, Fermi wavelength $\lambda_F=9.6$ nm). Using the Hall mobility ($\mu_H=9300$ cm^2/Vs), we obtained elastic mean free path: $l_{\text{mean}}=v_F\tau=404$ nm, where v_F is the Fermi velocity and $\tau=m^*\mu_H/e$ is the scattering time.

To fabricate a ballistic quantum wire, we patterned Hall-bar nanowires using the $Al_{0.18}Ga_{0.82}N/GaN$ heterostructure. The nanowires were prepared in two steps. The first step was to process a Hall bar pattern by inductively coupled plasma (ICP) dry etching with a chlorine versus nitrogen flowing rate of 10/10 SCCM (SCCM denotes standard cubic centimeter per minute at STP) and ICP versus rf power of 600/100 W at the pressure of 2 mtorr. The etching rate obtained was 166.7 nm/min. The geometry of the Hall-bar was designed as 20 μm width of active channel, 4800 μm length between source and drain, and 30 μm distance between voltage electrode leads. The second step was to reduce the width of active channel from 20 μm down to nanometer scales (200 nm in this study) along the $[11\bar{2}0]$ direction by a dual-beam focused ion beam (FIB) with a beam size of 60 nm for primary etch and 22 nm for fine etch. Before the FIB lithography, a 150 nm SiO_2 preservation layer was deposited on the surface by sputtering SiO_2 target under 4 mtorr argon gas pressure to avoid the damage from the ion beam. The depth of the FIB lithography was 300 nm measured from the SiO_2 preservation layer of the sample. After the FIB lithography, a 450 nm SiO_2 insulation layer was deposited on the quantum wires. The results of the FIB lithography are shown in Figs. 1(d)–1(f), where the dotted block of Fig. 1(d) was enlarged to Fig. 1(e). Figure 1(f) is the exampl of the final pattern of the nanowire. After the nanowire was fabricated, indium Ohmic contacts were annealed in a N_2 forming gas at 350 °C for 5 min. The Ohmic contacts of the nanowire were checked at room temperature to ensure the measurement of magnetoresistance.

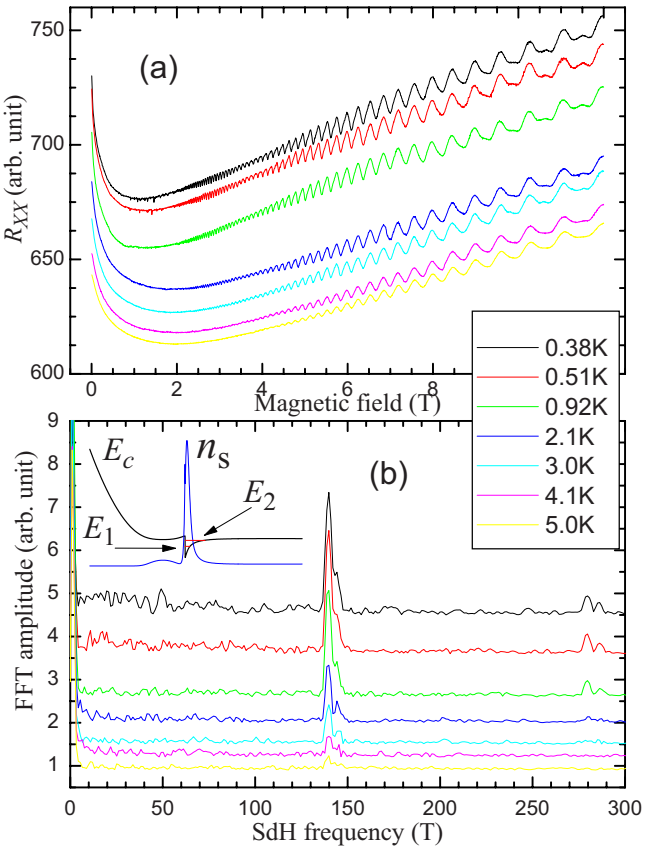

FIG. 2. (Color online) (a) The magnetoresistances of the nanowire against magnetic field for different temperatures. (b) The FFT spectra of the magnetoresistances in (a). The inset is the band profile of $Al_{0.18}Ga_{0.82}N/GaN$ heterostructure.

Figure 2(a) shows the magnetoresistance of the nanowire versus magnetic field at different temperatures, where the zeroes of y-axes were offset for comparison. The data points (1754 points) were taken from 0 to 12 T with a linear-field (B) increment, using ac modulation lock-in technique (modulation current $<10^{-5}$ A and ac frequency=80 Hz). It was found that the negative magnetoresistance presented at the low fields (e.g., <1 T) is induced by weak localization

effect,[15] while Shubnikov–de Haas (SdH) oscillations are detected at the field higher than 2 T. Since SdH oscillatory magnetoresistance is periodic in inversed filed $(1/B)$, we truncated the oscillatory magnetoresistance (from 1 to 12 T) and removed the monotonic background by the interpolation with an equal-spacing in $1/B$ to perform a fast Fourier transformation (FFT). The FFT spectra are shown in Fig. 2(b). In order to reconfirm the FFT results, we reran the magnetoresistance measurement by taking the data (2048 points from 0.25 to 12 T) with an equal-spacing of $1/B$ and performed the FFT program directly on the truncated oscillatory magnetoresistance (1 to 12 T). The results are highly consistent within the uncertainty of FFT frequency (0.56 T). In the FFT spectra, we found that the SdH frequency is split into two frequencies, $f_1=(139.8\pm0.6)$ T, and $f_2=(144.2\pm0.6)$ T. Both splitting frequencies faded away in the same manner as the temperature increased to 5.0 K and disappeared at 15.0 K. The temperature-dependent SdH beating patterns can eliminate the possibility of the magneto-intersubband resonant scattering,[16] in which the secondary peak is dominant at high temperatures when two subbands of 2DEG are populated. The two spin-splitting frequencies lead to the electron densities of $n_{2d}=(3.38\pm0.03)$ and $(3.49\pm0.03)\times10^{12}$ cm^{-2}, respectively, which is consistent with the calculated carrier concentration based on the van der Pauw measurement ($n_s=6.88\times10^{12}$ cm^{-2}). The spin-splitting energy calculated from the difference of the two spin carriers is (2.4 ± 0.3) meV.

The electron transportation in a nanowire heterostructure can be characterized by the mean free path (l_{mean}) as compared to its length (L) and width (W). When W and L are greater than the mean free path ($W,L>l_{\mathrm{mean}}$) the motion of the electron has a 2D character. As both W and L are smaller than the mean free path ($l_{\mathrm{mean}}>W,L$) the motion of electron exhibits a ballistic one-dimensional (1D) character, and an intermediate quasiballistic regime can be defined by the condition $L>l_{\mathrm{mean}}>W$ (e.g., our case). In a 2D diffusive channel, the electron transport follows the semiclassical Drude model, in which the quantum mechanical Fermi–Dirac statistic is taken into account while the dynamics of the electron motion at Fermi level is based on classical theory. However, the electron motion in a 1D ballistic wire is beyond the Drude model and should be described by quantum mechanics. When a magnetic field is applied to a nanowire, the electron trajectory can be classified as a cyclotron orbit, skipping orbit, or traversing trajectory, depending on the collision with none, one, or both confining walls, respectively, and denoted as magnetoelectric subbands.[17] In the quasiballistic region, the magnetoresistance exhibits an oscillation due to the depopulation of magnetoelectric subbands and Landau levels of cyclotron orbits. If the electron concentration is so large or the applied field is low enough that the Fermi level is constant as the field sweeps, the frequency of the oscillation will be equal to that of the SdH oscillation in 2DEG: $f_{\mathrm{SdH}}=hn_{2d}/se$, where $s=2$ for a spin-degenerate electron system and $s=1$ for a spin-splitting electron system. However, the amplitude of the magnetoresistance oscillation is smaller as compared to that of 2DEG due to the scattering from intersubbands or from the edge states, which occur at the intersection between the skipping and cyclotron orbits or traversing trajectories.[17] If an Aharonov–Bohm quantum-ring interferometer is made of a nanowire, the scattering from the edge states cannot be avoided when applied a magnetic field. However, the proposed spin-Hall quantum-ring interferometer benefits not only by the intrinsic large spin-splitting in GaN but also by the technical electric-gate-control (instead of magnetic-field-control) and the spin-current injection by the spin-Hall effect (instead of ferromagnetic electrodes).

In conclusion, we observed the spin splitting in a quasiballistic $Al_xGa_{1-x}N/GaN$ quantum wire. The spin-splitting energy calculated from the difference of the two spin carriers is (2.4 ± 0.3) meV. By replacing the host material InGaAs/AlInAs with an $Al_xGa_{1-x}N/GaN$ nanowire, the quantum-ring interferometer can be improved by a gated nanowire arm. A low-power spin-Hall quantum-ring interferometer would then be achieved by tuning the gate voltage on the gated arm. Unlike the Aharonov–Bohm quantum-ring interferometer, whose signal is modulated by a magnetic field due to the periodic phase dependence on magnetic flux (h/e), the signal of the spin-Hall quantum-ring interferometer would be controlled by the Rashba term with an electric-gate voltage.

The authors thank M. H. Gau, C. H. Hsieh, C. C Yang, R. Y. Su, and C. H. Chen for their assistance. The project was supported by National Science Council and Core Facilities Laboratory in Kaohsiung-Pingtung Area, Taiwan. The authors are also grateful to W. C. Mitchel and M. Mah for their help and AFOSR/AOARD, USAF for financial support under Grant No. FA4869-07-1-4022.

[1] L. P. Lévy, G. Dolan, J. Dunsmuir, and H. Bouchiat, Phys. Rev. Lett. **64**, 2074 (1990).
[2] V. Chandrasekhar, R. A. Webb, M. J. Brady, M. B. Ketchen, W. J. Gallagher, and A. Kleinsasser, Phys. Rev. Lett. **67**, 3578 (1991).
[3] D. Mailly, C. Chapelier, and A. Benoit, Phys. Rev. Lett. **70**, 2020 (1993).
[4] R. J. Warburton, C. Schäflein, D. Haft, F. Bickel, A. Lorke, K. Karrai, J. M. García, W. Schoenfeld, and P. M. Petroff, Nature (London) **405**, 926 (2000).
[5] D. Granados and J. M. García, Appl. Phys. Lett. **82**, 2401 (2003).
[6] Y. Aharonov and D. Bohm, Phys. Rev. **115**, 485 (1959).
[7] T. Raz, D. Ritter, and G. Bahir, Appl. Phys. Lett. **82**, 1706 (2003).
[8] X. Cartoixa, D. Z.-Y. Ting, and Y.-C. Chang, Appl. Phys. Lett. **83**, 1462 (2003).
[9] J. Wunderlich, B. Kaestner, J. Sinova, and T. Jungwirth, Phys. Rev. Lett. **94**, 047204 (2005).
[10] I. Lo, J. K. Tsai, W. J. Yao, P. C. Ho, L. W. Tu, T. C. Chang, S. Elhamri, W. C. Mitchel, K. Y. Hsieh, J. H. Huang, H. L. Huang, and W. C. Tsai, Phys. Rev. B **65**, 161306 (2002).
[11] I. Lo, M. H. Gau, J. K. Tsai, Y. L. Chen, Z. J. Chang, W. T. Wang, J. C. Chiang, T. Aggerstam, and S. Lourdudoss, Phys. Rev. B **75**, 245307 (2007).
[12] W. T. Wang, C. L. Wu, S. F. Tsay, M. H. Gau, I. Lo, H. F. Kao, D. J. Jang, J. C. Chiang, M. E. Lee, Y. C. Chang, C. N. Chen, and H. C. Hsueh, Appl. Phys. Lett. **91**, 082110 (2007).
[13] J. Sinova, D. Culcer, Q. Niu, N. A. Sinitsyn, T. Jungwirth, and A. H. MacDonald, Phys. Rev. Lett. **92**, 126603 (2004).
[14] M. Grundmann, BandEng Alpha Version 2003, mgrundmann@ece.ucsb.edu
[15] I. Lo, S. J. Chen, L. W. Tu, W. C. Mitchel, R. C. Tu, and K. Y. Su, Phys. Rev. B **60**, R11281 (1999).
[16] I. Lo, J. K. Tsai, M. H. Gau, Y. L. Chen, Z. J. Chang, W. T. Wang, J. C. Chiang, K. R. Wang, C. N. Chen, T. Aggerstam, and S. Lourdudoss, Phys. Rev. B **75**, 245307 (2006), and references therein.
[17] C. W. J. Beenakker, H. van Houten, and B. J. van Wees, Superlattices Microstruct. **5**, 127 (1989).